CoA Memo. No. 130

July, 1967

THE COLLEGE OF AERONAUTICS

DEPARTMENT OF PRODUCTION AND INDUSTRIAL ADMINISTRATION

A new approach to the prediction of tool wear

- by -

J. Cherry, M.Sc.

SUMMARY

Cutting tests were conducted on EN8b and EN9 materials which have led to the following hypothesis 'For a given tool and workpiece combination the wear on the rake face of the tool is proportional to the work done in friction'.

Further tests are being undertaken to determine the limits of application of this hypothesis.

1.0 Introduction

Tool life is of major concern for economical production in the metal cutting industries and a simple method of predicting the tool wearability of materials would be of considerable value in enabling optimum cutting conditions to be determined.

It has been shown[1] that tool life for minimum cost per piece = $(\frac{1}{n} - 1)K$ where 'n' is the exponent in the speed/life relationship $VT^n = C$.

Since 'n' is substantially constant for a given tool material and chip thickness, and K is constant for given operating conditions then the life of the tool (T) has an unique value under these circumstances. Also since tool life (T) will be determined by a specific magnitude of tool wear, a simple method by which the time to arrive at this criterion could be predicted would be very useful. In the experimental work to be described it has been possible from simple cutting tests to predict tool wear over a limited range of conditions. Much more extensive research is required to establish the range of the technique.

In metal cutting processes where tool wear is the criterion of tool life, wear may be caused by various factors e.g.

(a) ploughing by hardened metal or inclusions[2]

(b) shearing of the welds between chip and tool[2]

(c) diffusion of tool material into the chip[3,4].

Ploughing by hardened metal occurs predominantly at slow speeds when a built up edge is formed, and wear by diffusion occurs predominantly at high speeds where temperatures are high. Between these extremes is the normal cutting speed zone where wear is mainly caused by shearing:

It is to this practical zone that the present technique is confined.

In the course of an investigation into oblique machining[2] a series of experiments was conducted on test material EN8b using a tungsten titanium carbide tool to examine the relationship between the work done on friction on the rake face of the tool and the actual wear of the tool. High correlation was established and led to the hypothesis 'For a given tool and workpiece combination the wear on the rake face of the tool is proportional to the work done in friction'.

Tests were extended to a second material EN9 and high correlation was found between EN8b and EN9 materials. Further tests are being undertaken to determine the limits of application of this hypothesis.

2.0 Experimental procedure for cutting force measurement

2.1 Dynamometer

As previously mentioned the original test programme was to investigate oblique machining (as illustrated in Fig. 1), with particular reference to cutting forces and tool wear. Since the validity of any conclusions would depend on the accuracy of the test results, considerable attention was paid to the design, manufacture and calibration of a three-dimensional dynamometer for use on a lathe. The instrument in position on the machine is shown in Fig. 2 and a diagram of the principle of operation is shown in Fig. 3.

In the calibration of the dynamometer the conventional method of independent loading in each of the three principal directions was not considered sufficient, as this gives no guarantee of accurate resolution of the single cutting force during the machining operation, hence an additional technique was employed as shown in Fig. 4 in which an oblique force was applied to simulate the actual force experienced during the cutting operation.

Oblique forces were applied to cover the range in which the actual cutting forces were expected to occur as illustrated in Fig. 5 and deflections recorded in the vertical, F_c, side F_t and radial F_1, directions. From the known oblique forces, the corresponding forces in the vertical side and radial directions were calculated and a calibration chart drawn as shown in Fig. 6. As will be observed the variations in values over the wide range of loading is quite small, the mean deviations being as follows:-

Vertical force	$F_c = 2.5\%$
Side force	$F_t = 1.5\%$
Radial force	$F_1 = 2\%$

These results were considered very satisfactory and average curves computed by the least squares method were drawn as shown in Fig. 7 and used for conversion purposes.

2.2 Cutting forces

The range of tools used during the test is shown in Fig. 8 and the experimental set-up is shown in Fig. 2. Diagrammatic representation of the position of the tools relative to the workpiece is shown in Fig. 9.

All tools had 30° primary rake (normal to the cutting edge) and 5° true clearance. Surface finish in all cases was less than 5 C.L.A.

Tests were conducted for each tool at .0025" and .005" feed per rev employing a cutting speed of 70 f.p.m. The magnitude and direction of the resultant force (cutting force) was calculated as shown in Fig. 10 and results are given in Figs. 11 and 12.

Examination of these results will reveal that the angle 'O' (the angle the cutting force R_2 makes with R_1) is approximately half the angle of obliquity 'γ' e.g.

Obliquity	.0025" Feed/rev angle 'O'	.005" Feed/rev angle 'O'
30°	15°29	15°20
45	24°14	25°19
60°	29°30	30°7

2.3 Energy relationships

As shown by E. Merchant[2] the total work done in cutting W_c is composed of the sum of the work done in shear W_s and the work done in friction W_f.

$$W_s = S_s \epsilon$$ Work done in shear W_s per unit volume

where S_s = shear stress

ϵ = shear strain

In oblique machining

$$S_s = \frac{\text{Sin } \phi \text{ Cos } \gamma(F_c \text{ Sin } \gamma - F_1 \text{ Cos } \gamma)}{A_o \text{ Sin } \delta}$$

where δ = angle of shear stress

also $$\text{Tan } \phi = \frac{r_t \text{ cos } \alpha}{1 - r_t \text{ Sin } \alpha}$$

r_t = cutting ratio $= \frac{t_1}{t_2}$

and $$\text{Tan } \delta = \frac{\text{Tan } \gamma \text{ Cos}(\phi - \alpha) - \text{Tan } \beta \text{ Sin } \phi}{\text{Cos } \alpha}$$

γ = angle of obliquity

β = angle of chip flow

therefore in order to obtain reliable values of shear stress it was necessary to be able to measure r_t and β with a high degree of accuracy. To enable this to be done a new technique was devised in which the test piece was prepared as shown in Fig. 13 and mounted on a vertical broaching machine as shown in Fig. 14. The test piece is machined with a number of slots to make each cutting length equal at 1". Typical chips produced by this technique are shown in Fig. 15.

By rubbing a chip on an ink pad and rolling it subsequently on paper the developed shape of the chip can be ovtained as shown in Fig. 16.

Measurement can then be made of the width of the chip after cutting W_2, and the length of the chip after cutting L_2. Examination of Fig. 16 will

also reveal that the ends of the chip are not square with the sides but form an angle approximating to half the angle of obliquity. This feature is used as a check on the accuracy of measurement of W_2 and L_2 since the distance across the corners of the chip C_1 (Fig. 16) can be measured as shown in Fig. 17 and used to calculate the angle 'e' of the end of the chip. agreement between calculated 'e' and measured 'e' would indicate correct values. Having verified such measurement and knowing the original volume of the chip then the chip thickness ratio r_t can be obtained as shown in Fig. 18. The angle of chip flow is found as follows:-

$$\text{Cos } \beta = \frac{W_2}{W_1} \text{ Cos } \gamma$$

A summary of the results of these calculations is shown in Fig. 19. Examination of these results show close agreement with the angle of chip flow ' ' as obtained by G. Stabler [3,4,5].

Work done in Friction W_f per unit volume

$$W_f = \frac{Fr_t}{Ao}$$

For orthogonal machining

$$F = F_t \cos \alpha + F_c \text{ Sin } \alpha$$

For oblique machining

$$F = \frac{F_c \sin \gamma - F_1 \cos \gamma}{\text{Sin } \beta}$$

A summary of the results obtained is given in Fig. 20. A graph of Force/Energy V_s Angle of obliquity is given in Fig. 21. It will be observed that the work done in friction is a minimum at 30° obliquity.

3.0 Wear Tests

Cutting tests were conducted to investigate the effect of the angle of obliquity on the wear of both flank face and rake face of the tool as illustrated in Fig. 22.

The measurement criteria adopted were as follows:-

Flank - True wear

Preliminary tests showed that rapid wear and final breakdown for each of the four angles of obliquity occurred when true wearland, as measured in

the direction of cut, reached a critical magnitude and that wearland measured normal to the cutting edge was not a general criterion; therefore true wearland was chosen as the criterion for flank wear. To obtain the values for true wearland, direct measurement was made of the normal wearland as shown in Fig. 23 which was then converted to true wearland as shown in Fig. 24.

Volume of Flank Wear

From the calculations so established for true flank wearland, calculations were made to establish the volume of flank wear as illustrated in Fig. 25.

Rake Face

The volume of material worn from the rake face of the tool as illustrated in Fig. 22 was chosen as the criterion for wear on the rake face. To obtain this volume the contour of the crater was traced on a Talysurf Surface Finish instrument using the datum attachment and measurements were made of the depth and width of crater from which the volume was calculated.

Test procedure

Wear tests were conducted using a square tool as shown in Fig. 26 mounted in a toolholder which permitted angular setting of the tool. All four angles of obliquity 0°, 30°, 45° and 60° could then be tested on one end of the tool. Radial adjustments were made to the setting angle for each angle of obliquity in order to maintain uniform width of chip. The external diameter of the workpiece was machined by each tool in a randomised sequence. Measurements were made of the progression of both the flank wearland and the crater contour.

Flank Wear

Normal flank wearland was measured after each edge had cut one length of the workpiece. From these results the true wearland W_t was calculated, also the volume lost by wear.

A summary of these results is shown in Fig. 27. A graph of True Flank Wearland V_s Time is shown in Fig. 28 and Fig. 29 shows a graph of Flank Wear (Volme) V_s Time. It will be observed that least wear occurs when the tool is set at 30° obliquity.

Crater Wear

After each test run a trace of the crater contour formed normal to the cutting edge was taken as shown in Fig. 30. From each trace the depth of crater 'h' and the width of crater 'c' were measured. In the cases of 30°, 45° and 60° angle of obliquity the normal width of crater was converted to give the true width of crater in the direction of cutting thus keeping the

volumetric relationship comparable. A summary of the results is given in Fig. 31. These results are shown graphically in Fig. 32. It will be observed that least wear occurs when the tool has 30° obliquity.

From the Talysurf traces of the crater wear as shown in Fig. 30, a graph was drawn as shown in Fig. 33 to illustrate the growth of wear for each cutting edge. It will be observed that the width of crater remained substantially constant throughout the test period, although the depth of crater increased progressively.

A graph showing the volume of metal removed in relation to angle of obliquity is shown in Fig. 34. Again it is seen that minimum wear occurs at 30° obliquity.

4.0 Comparison of wear with work done in friction

Comparison of this curved with the curve in Fig. 21 showing the work done in friction is made in Fig. 35 whence it will be observed that there is considerable correspondence between these curves which gives rise to the hypotheses 'For a given work material and tool material combination under identical cutting conditions the volume of metal removed from the rake face of the tool is proportional to the work done in friction'. To test this hypotheses further, a series of tests was conducted on EN9 material to measure the work done in friction W_f for the range of angles of obliquity previously used; these tests were followed by wear tests on the 0° tool and comparison made with the results obtained from the EN8b material.

A summary of the cutting force measurements and the work done in friction is given in Fig. 36. A graph of work done in friction V_s Angle of obliquity is shown in Fig. 37.

The results of crater wear are shown in Fig. 38 and a graph of these results is shown in Fig. 39. A similar wear pattern as for EN8b is obtained.

Comparison of these results for EN9 material with the results EN8(b) material give the following relationship.

	EN8(b) Bhn 164	EN9 Bhn 205	Ratio
Work done in Friction W_f	107,000	132,000	1.23
Crater volume after 10 mins.	2.8×10^{-6}	3.4×10^{-6}	1.22

From which it will be seen that the ratio of the work done in friction approximates to the ratio of crater volume hence support is given to the extension of the hypotheses to read 'For a given tool material and work material of similar composition under identical cutting conditions the volume of metal removed from the rake face is proportional to the work done in friction'.

Obviously much more work will be required to substantiate this hypothesis and to establish the limits of variation in material composition which can be tolerated within one family group also the relationships between family groups.

However, the usual criterion which determines tool life is flank wearland and comparison was made between the flank wear produced when machining EN8b and when machining EN9 under identical conditions.

No direct measurement was made of the work done in friction on the flank face but it would be reasonable to assume the following relationship:-

$$\frac{W_f \text{ Rake Face (EN9)}}{W_f \text{ Rake Face (EN8b)}} = \frac{W_f \text{ Flank (EN9)}}{W_f \text{ Flank (EN8b)}} = \frac{\text{Flank Wearland (EN9)}}{\text{Flank Wearland (EN8b)}}$$

To test this assumption measurements were made of the width of flank wearland when machining EN9 with an orthogonal tool (obliquity = 0°) and these are charted on Fig. 40.

Examination of the curves of flank wearland when machining EN8b shown in Fig. 28 reveal the equation to be of the form $mT + C$ and the wearland for 0° tool after 12 minutes cutting is .0087".

Applying the relationship:

$$\frac{\text{Flank wearland EN9}}{\text{Flank wearland EN8b}} = \frac{W_f \text{EN9}}{W_f \text{EN8b}}$$

then Flank Wearland EN9 = Flank Wearland EN8b x 1.23

$$= .0087 \times 1.23$$

$$= .0107$$

Reference to Fig. 40 will show the actual wearland as .011" which is in very close agreement.

5.0 Conclusions and Recommendations

From the results of these tests it is apparent that for the materials used (EN8b and EN9) it can be stated 'For a given tool and work material of similar composition under comparable cutting conditions the volume of metal removed from the rake face of the tool is proportional to the work done in friction on the rake face'.

It is suggested that further investigation into a machinability/wearability index based on the relationship of work done in friction would be fruitful and might lead to a practical quantitative index.

6.0 List of symbols

α = normal rake angle of tool

β = angle of chip flow

ϕ = angle of shear plane

γ = angle of inclination of cutting edge

δ = angle between direction of shear of metal on shear plane and a perpendicular to the cutting edge of tool, as measured in plane of surface generated

ϵ = shearing strain undergone by chip

μ = coefficient of friction acting between sliding chip and tool face.

F_c = cutting force

F_t = thrust force

R = resultant force

V = cutting speed (feet/min)

T = tool life (mins.)

7.0 References

1. W.W. Gilbert — 'Economics of Machining'
2. Bowden and Tabor — The Friction and Lubrication of Solids.
3. E.M. Trent — Some Factors affecting wear on cemented carbide tools.
4. H. Opitz and M. Gappisch — Some recent research of the wear behaviour of carbide cutting tools.
5. M.E. Merchant — 'Mechanics of the Metal Cutting Process'.
6. G.V. Stabler — 'The Basic Nomenclature of Cutting Tools'.
7. G.V. Stabler — 'The Chip Flow Law and its consequences'.

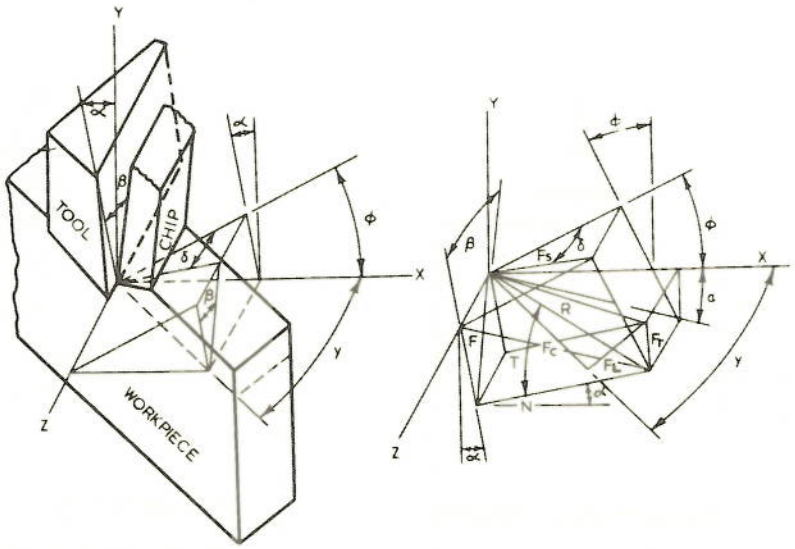

FIG.I. OBLIQUE MACHINING.

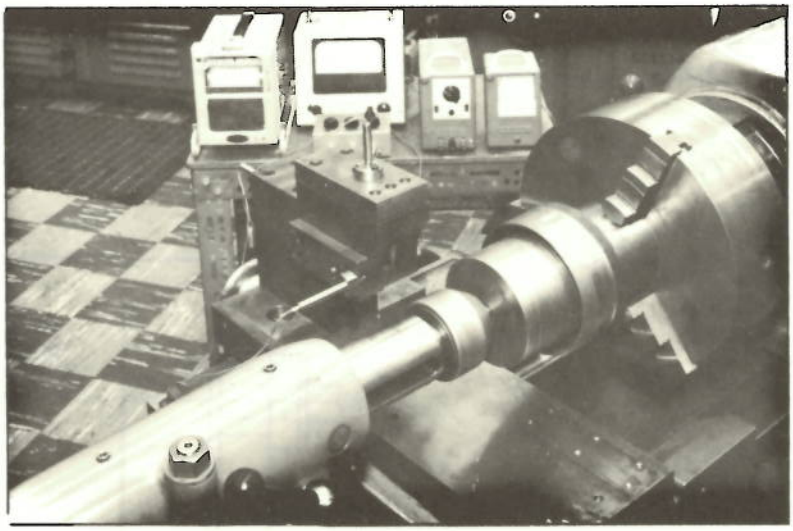

FIG. 2 EXPERIMENTAL SET UP FOR MEASUREMENT OF CUTTING FORCES

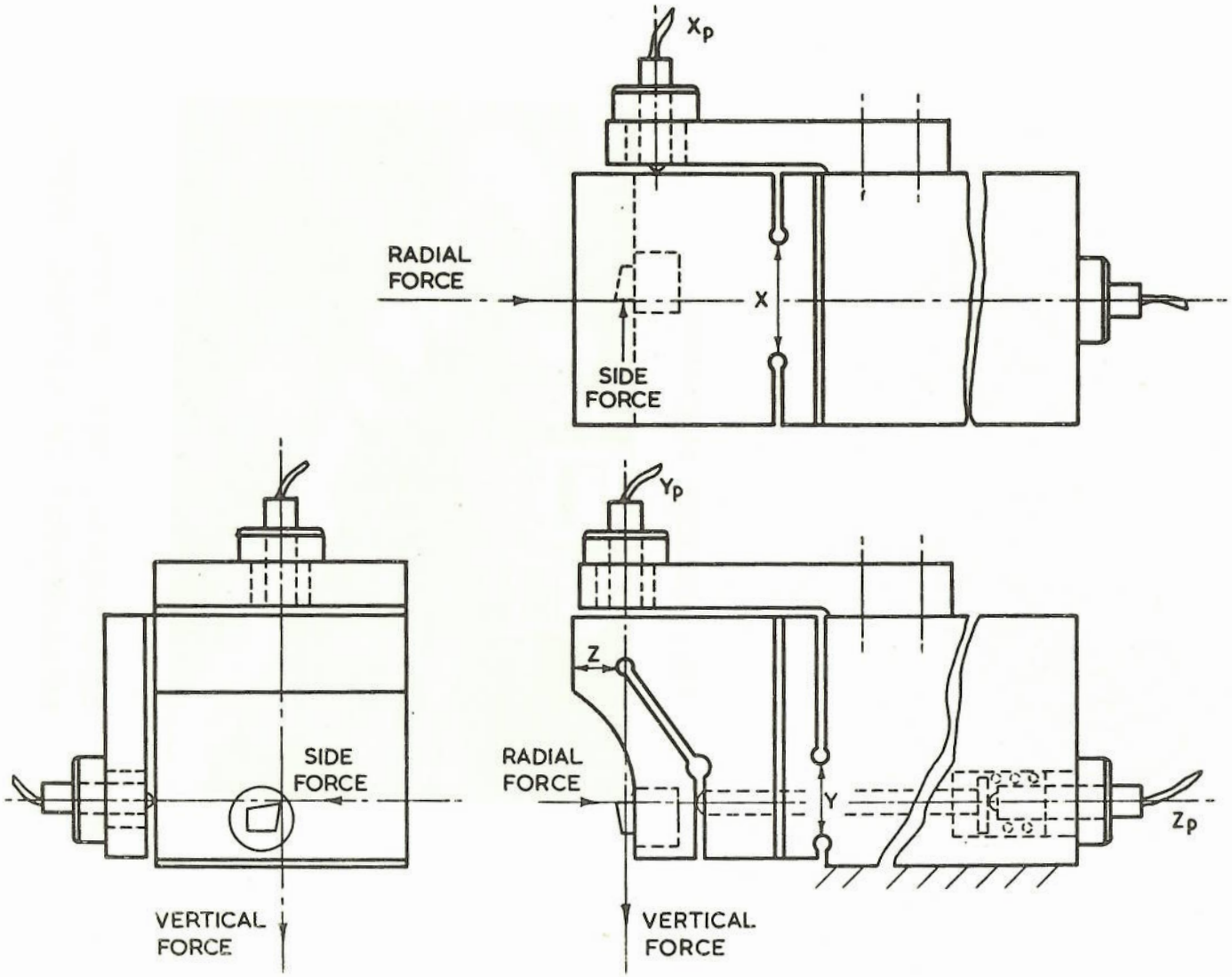

FIG.3. 3 COMPONENT DYNAMOMETER.

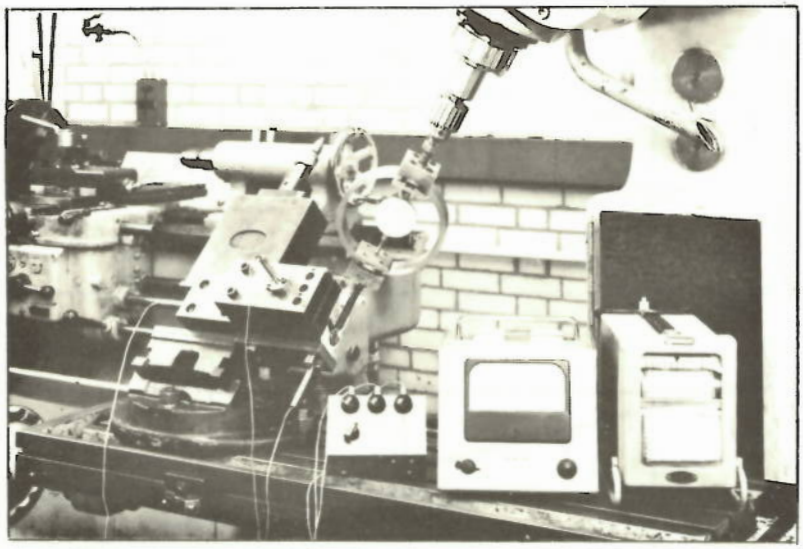

FIG. 4 METHOD OF APPLYING OBLIQUE LOAD TO DYNAMOMETER

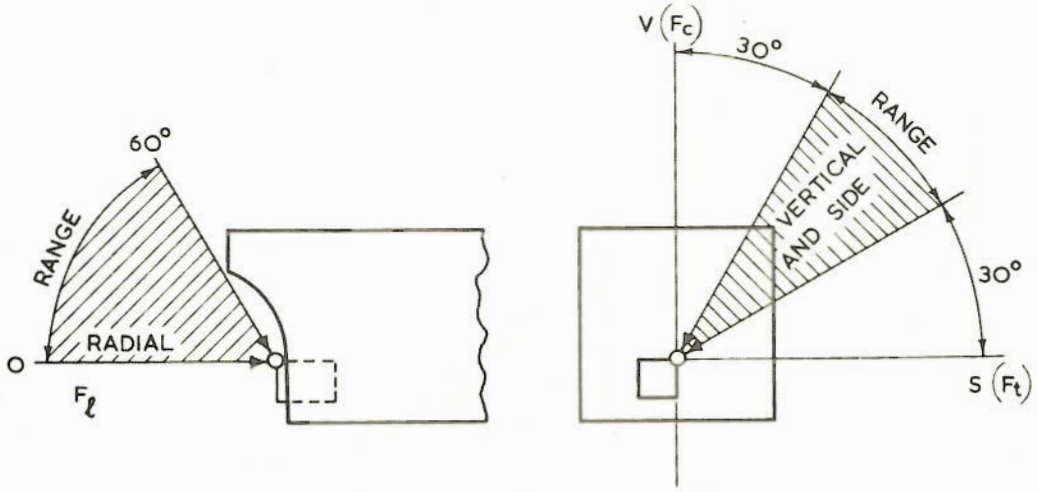

RANGE OF OBLIQUE LOADS APPLIED

	TEST .1.	TEST .2.	TEST .3.
(F_c)	V 30°	V 45°	V 60° ALSO R = 0°
(F_t)	S 60°	S 45°	S 30°
(F_ℓ)	R 60°	R 60°	R 60°

FIG.5. OBLIQUE LOADING.

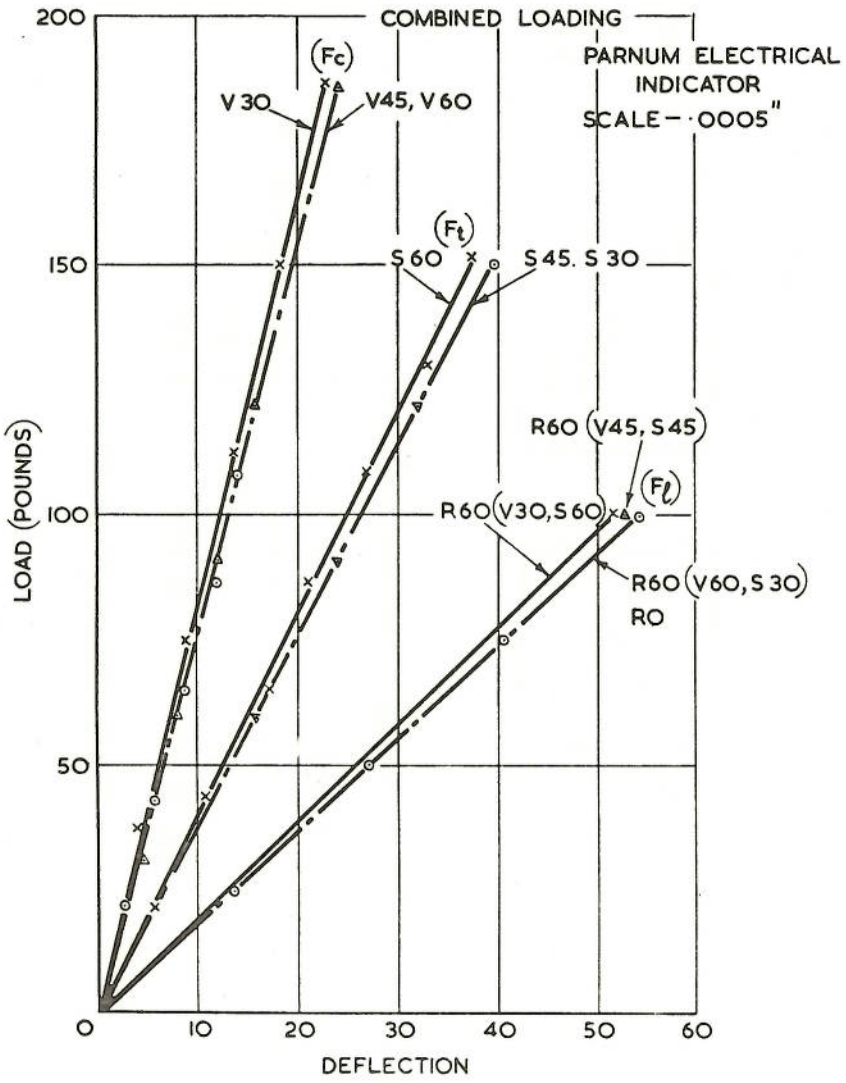

FIG.6. CALIBRATION OF CANTILEVER DYNAMOMETER

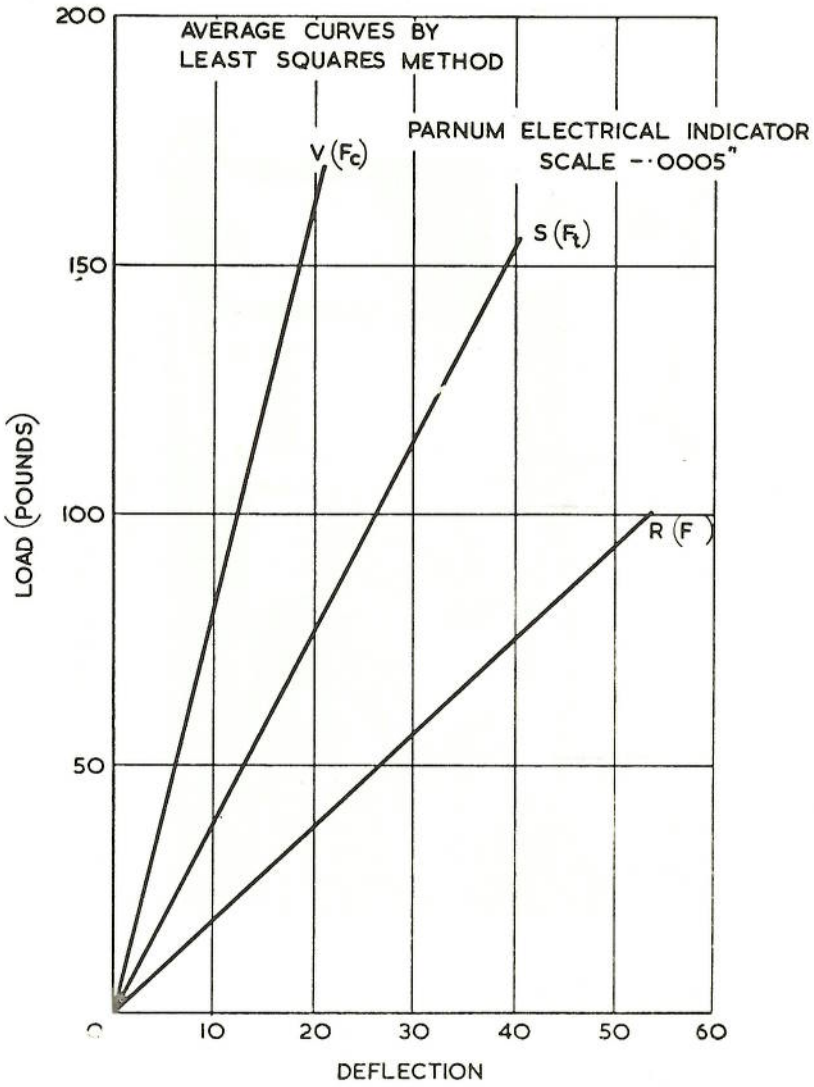

FIG.7. CALIBRATION OF DYNAMOMETER COMBINED LOADING.

FIG. 8 RANGE OF TOOLS USED FOR FORCE MEASUREMENT

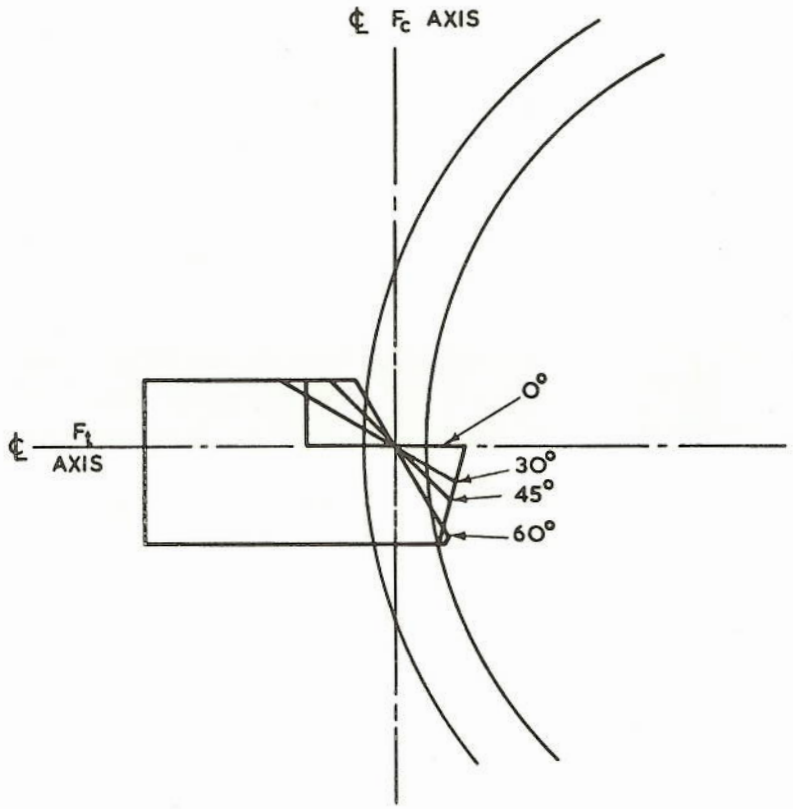

THE CUTTING EDGE OF ALL TOOLS IS ON THE ℄ OF THE F AXIS.

FIG.9. CUTTING POSITION OF TOOLS.

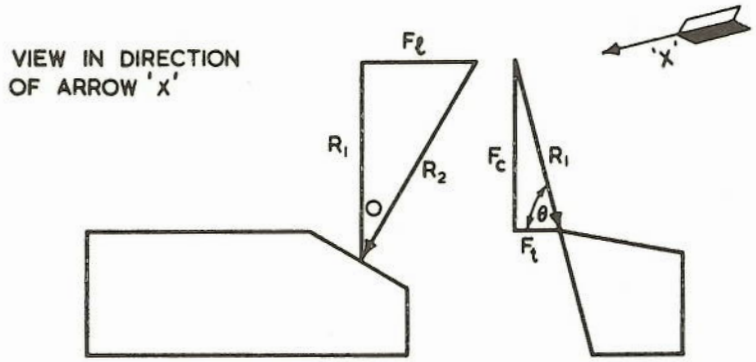

FIG.10. DIAGRAM OF FORCES RELATIONSHIP.

FIGURE 11

Calculations for Resultant Forces

Refer to diagram in Appendix A3.74

.0025" Feed/rev.

	0°	30°	45°	60°
Fc (lbs)	56	52	57	72
ft (lbs)	35	40	34	60
Cot $\measuredangle\theta$	.625	.754	.596	.833
$\measuredangle\theta$	58°	53°	59°12'	50°12'
R_1 = Ft Cosec θ (lbs)	66	65	66.8	93.6
F_L (lbs)	0	17	30	53
Tan $\measuredangle 0$	=	$\frac{17}{65}$	$\frac{30}{66.8}$	$\frac{53}{93.6}$
	=	.277	.45	.566
$\measuredangle 0$		15°29'	24°14'	29°30'
$R_2 = F_L \cos \measuredangle 0$		17 x 3.95	30 x 2.436	53 x 2.0308
(Lbs)		67	73	107

FIGURE 12

Calculations for Resultant Forces

(Refer to Diagram in Appendix A3.74)

.005" Feed/rev.

	0°	30°	45°	60°
Fc (lbs)	89	89	95	130
Ft (lbs)	65	57	54	123
Cot $<\theta$	.73	.64	.60	.948
$<\theta$	53°52	57°23	59°	46°32
R_1=Fc Cosec θ	89x1.238	89x1.187	95x1.167	130x1.378
(lbs)	110	106	110	179
F_L	0	28	52	104
Tan $<0 = \frac{F_L}{R_1}$		$\frac{28}{106}$	$\frac{52}{110}$	$\frac{104}{179}$
=		.274	.473	.58
<0 =		15°20	25°19	30°7
R_2 F_L cosec <0		28x4.049	52x2.3385	104x1.993
= (lbs)		113	122	207

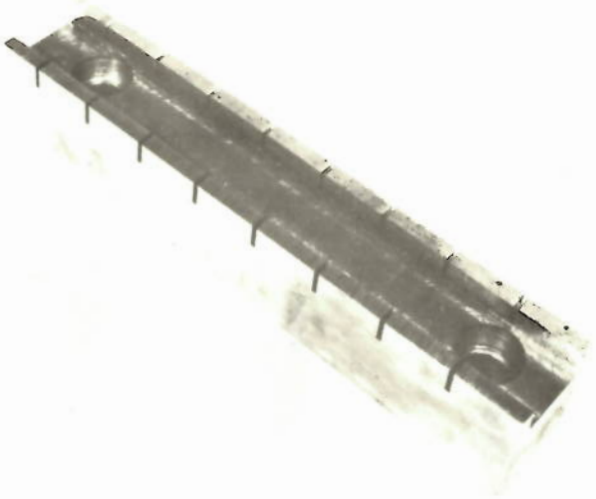

FIG. 13 TEST PIECE FOR BROACHING MACHINE

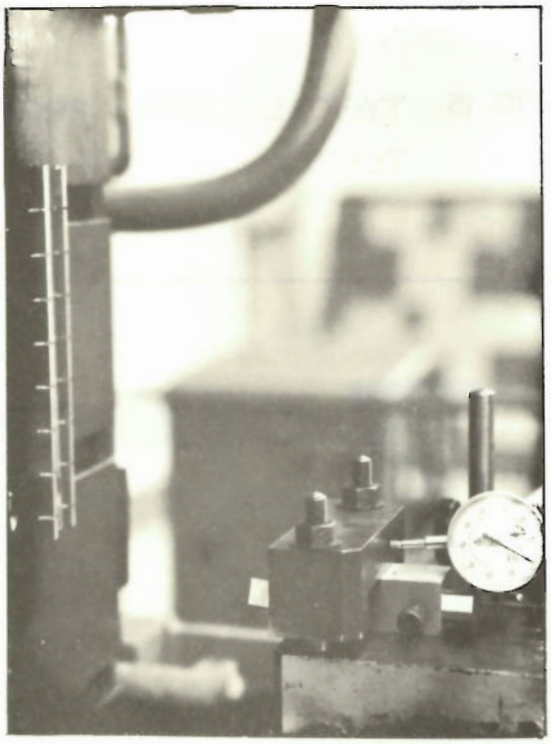

FIG. 14 EXPERIMENTAL SET-UP ON BROACHING MACHINE

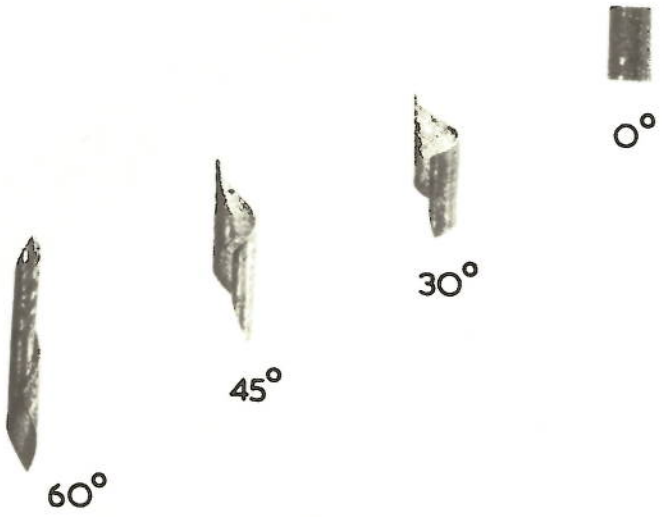

FIG. 15 TYPICAL CHIPS FROM BROACHING TESTS

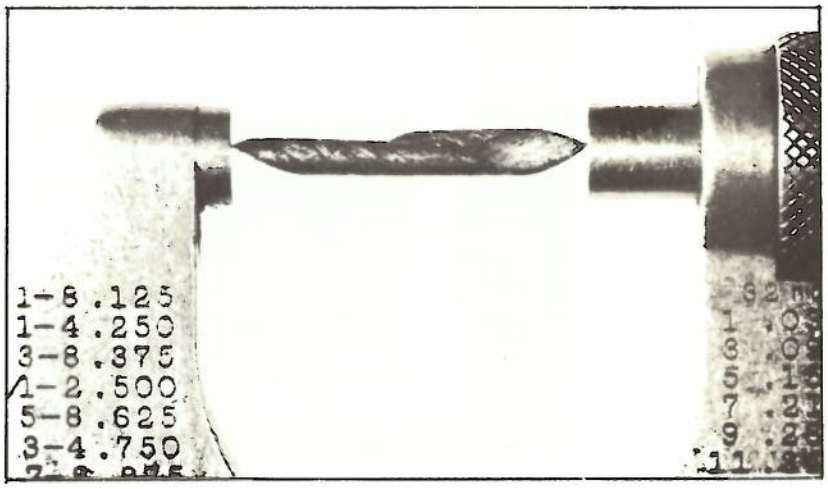

FIG. 17 MEASUREMENT ACROSS CORNERS OF CHIP

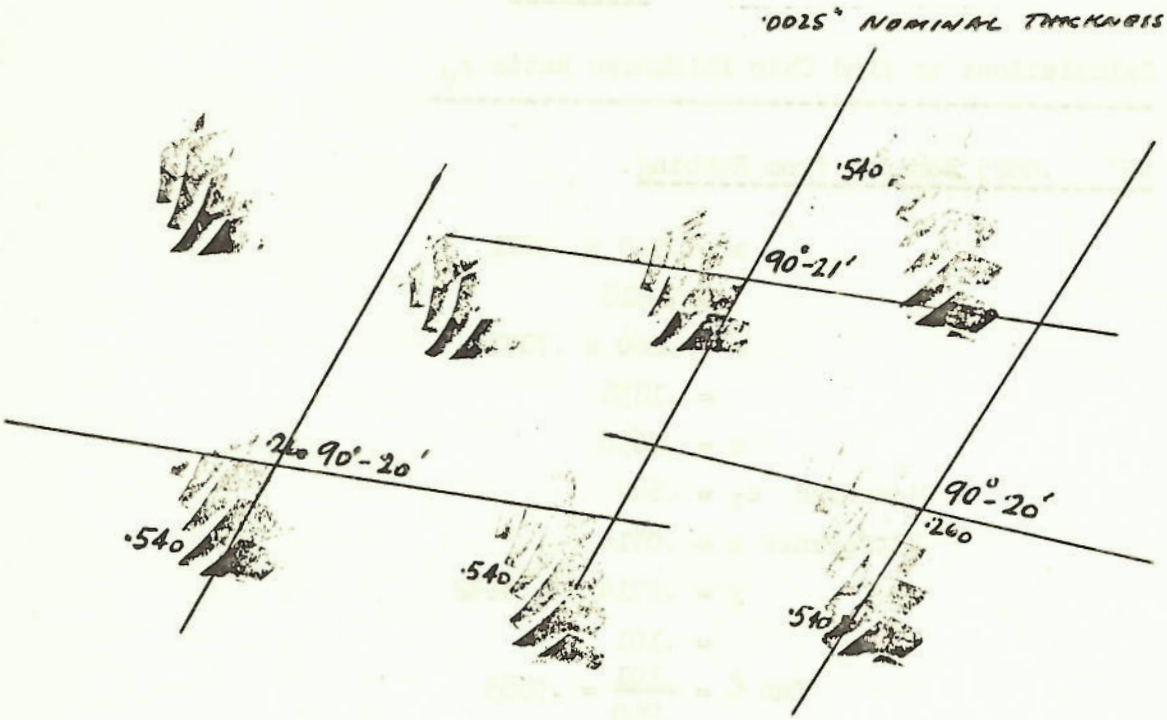

ORIGINAL WIDTH = .250"
FINAL WIDTH = .260"
" LENGTH = .540"
END ANGLE 'e' = 20°

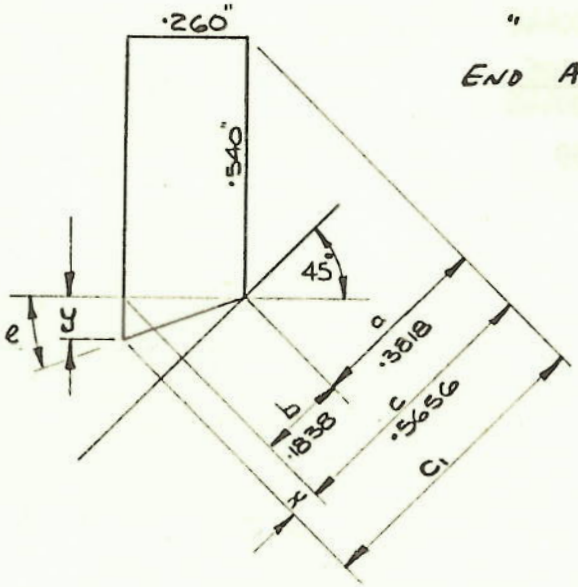

FIG. 16. DEVELOPED SHAPE OF CHIP 45°

FIGURE 18

Calculations to find Chip Thickness Ratio r_t

45° .0025 Nominal from Rubbing.

$$a = .540 \times .7071$$
$$= .3818$$
$$b = .260 \times .7071$$
$$= .1838$$
$$c = .5656$$
Measured $c_1 = .647$

Difference $x = .0714$

$$y = .0714 \times 1.4142$$
$$= .101$$
$$\text{Tan } \ell = \frac{.101}{.260} = .3883$$
$$< \ell = 21°13$$

$$t_2 = \frac{.0006273}{.260 \times .540}$$
$$= .00446$$
$$rt = \frac{.0026}{.00446}$$
$$= .59$$

FIGURE 19

Summary

Oblique Cutting Force Measurements

Speed: 70 PPM Parnum Gauge Scale: .0005"

(refer to diagram in Appendix A3.74)

Feed .0025 Wall thickness .104/.107

	0°		30°		45°		60°	
	Defl	lbs	Defl	lbs	Defl	lbs	Defl	lbs
V(Fc)	6.85	56	6.33	52	7	57	8.88	72
S(FT)	9.33	35	10.33	40	9	34	15.5	60
R(FL)	0	0	8.66	17	16	30	29.67	53
	58°		55°		59°12		50°12'	
R_1		65		65		66.8		93.6
R_2				67		73		110
<0				15°29'		24°14'	30°50'	
<e				13°15'		21°13'	28°17'	
<δ				19°3'		27°46'	31°3	
				28°		42°40	58°	

Feed .005 Wall thickness .100/.104

V(Fc)	11	89	11	89	12	98	16	130
S(FT)	17	65	15	57	14	54	32	123
R(FL)	0	0	14	27	28	52	56	104
	53°12'		57°23'		59°		46°32'	
R_1	110		106		110		179	
R_2			110		122		207	
<0			15°21'		25°19'		30°7'	
<e			13°45'		23°37'		28°32'	
<δ			19°6'		26°19'		30°32'	
<β			28°		43°52'		58°40'	

FIGURE 20

Summary of work done in Friction W_f per unit volume

.0025" feed/rev.

0°	30°	45°	60°
107,000	52,000	61,000	110,000

.005" feed/rev.

100,800	45,806	49,865	93,115

Summary of work done in Shear W_s per unit volume

.0025" feed/rev.

97,430	104,559	110,337	136,618

Total work done in Cutting $W_c = W_f + W_s$ per unit volume

.0025" feed/rev.

210,701	156,559	171,291	247,618

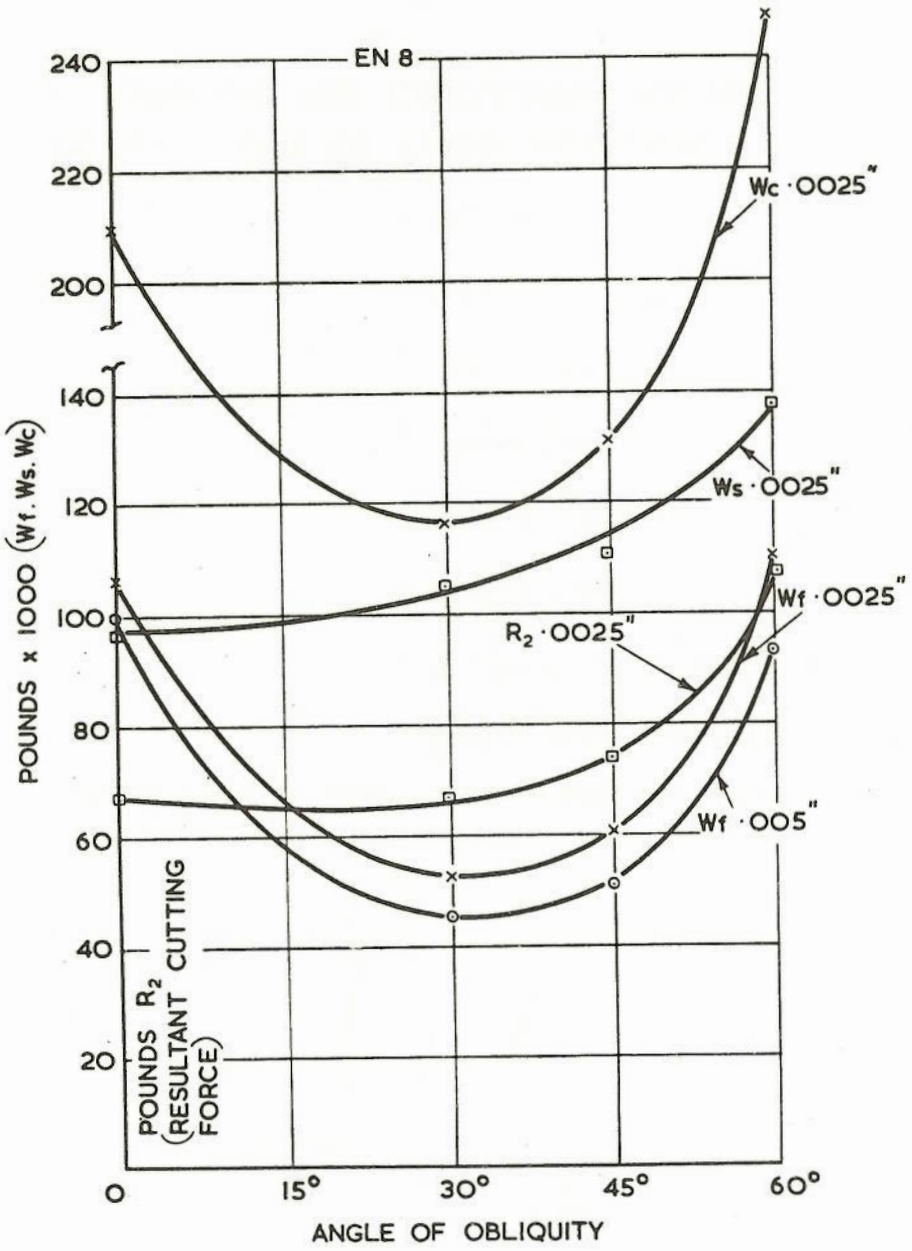

FIG.21. FORCE/ENERGY Vs ANGLE OF OBLIQUITY

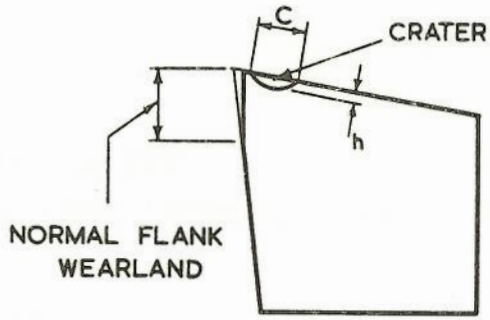

FIG. 22. WEAR CRITERIA.

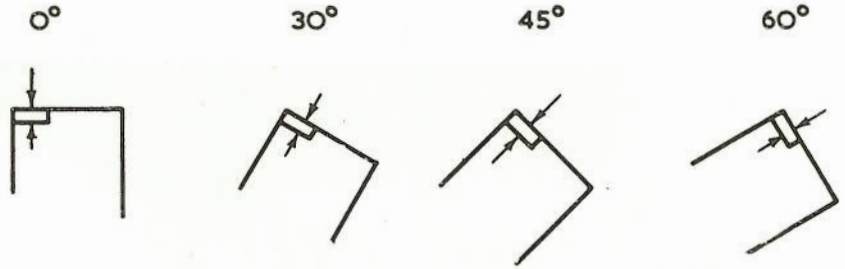

FIG.23. FLANK WEARLAND NORMAL TO CUTTING EDGE.

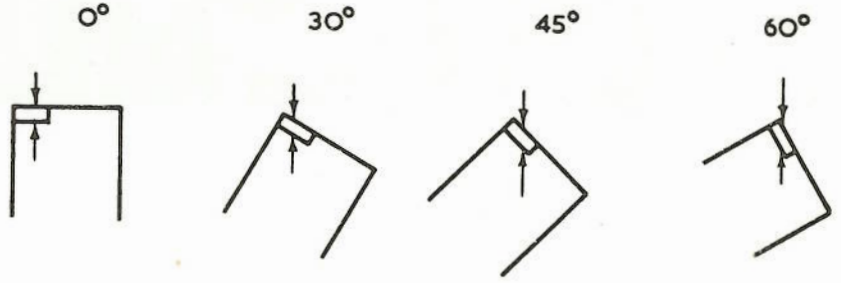

FIG.24. TRUE FLANK WEARLAND IN DIRECTION OF CUTTING.

OBLIQUITY 0°

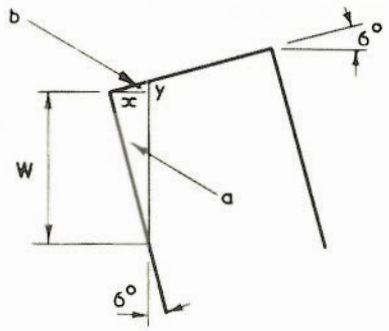

VOLUME OF FLANK WEAR = (AREA 'a' + AREA 'b') x LENGTH OF CUT

$$= \left(\frac{W \times x}{2} + \frac{x \times y}{2}\right) \times \text{CONSTANT (ASSUME 1)}$$

$$= \frac{W^2 \times \text{Tan } 6^\circ}{2} + \frac{x^2 \times \text{Tan } 6^\circ}{2}$$

$$= \frac{\text{Tan } 6^\circ \left(W^2 + x^2\right)}{2}$$

$$= \frac{\text{Tan } 6^\circ \left(W^2 + W^2 \text{ Tan}^2 6^\circ\right)}{2}$$

$$= \frac{\cdot 1051 \left(W^2 + W^2 \cdot 011\right)}{2}$$

$$= \frac{\cdot 1051 \times 1 \cdot 011 \, W^2}{2}$$

$$= \frac{\cdot 10626 \, W^2}{2}$$

$$= \cdot 05313 \, W^2$$

FIG.25. VOLUME OF FLANK WEARLAND FORMULAE FOR CALCULATING VOLUME.

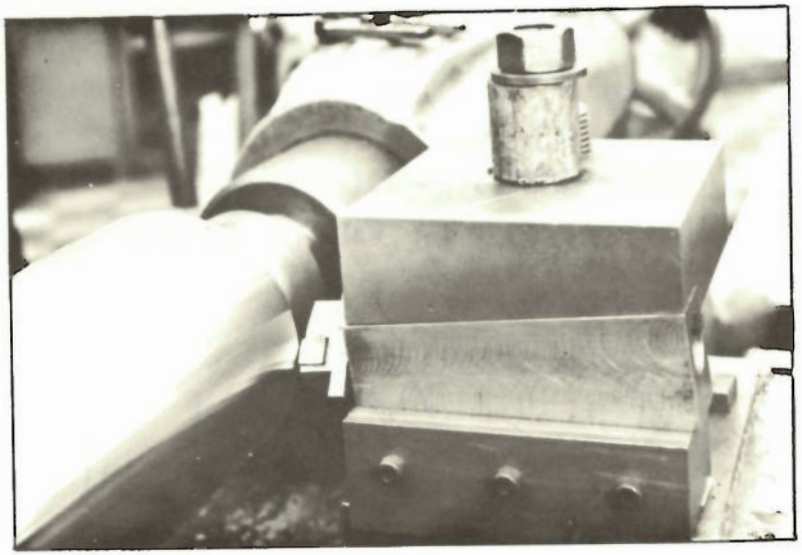

FIG. 26

TOOL AND ADAPTOR FOR PROLONGED WEAR TESTS

FIGURE 27

True Wearland and Flank Volume ($.0531W_1^2$)

EN8 TOOL No. 4 END A

True Wearland W_1 =		W	1.1547W	1.4142W	2 x W
Time (mins) Edge		1	2	3	4
3.5	W	.005	.0025	.0025	.002
	W_1	.005	.003	.0035	.004
	Vol	.00000135	.00000048	.00000065	.00000085
7	W	.006	.004	.004	.0032
	W_1	.006	.0046	.006	.0064
	Vol	.00000190	.00000122	.00000192	.00000218
10.5	W	.0075	.006	.0055	.004
	W_1	.0075	.007	.0075	.008
	Vol	.00000300	.00000260	.000003	.00000340
14	W	.010	.007	.0068	.0048
	W_1	.010	.008	.0096	.0096
	Vol	.00000531	.00000340	.00000490	.00000490
17.25	W	.011	.008	.008	.006
	W_1	.011	.0092	.011	.012
	Vol	.00000640	.00000450	.0000064	.00000762
20.5	W	.012	.0085	.0085	.0065
	W_1	.012	.010	.012	.013
	Vol	.0000076	.00000531	.0000076	.00000890
23.75	W	.014	.009	.009	.0075
	W_1	.014	.0104	.013	.015
	Vol	.00001042	.00000576	.00000890	.00001190

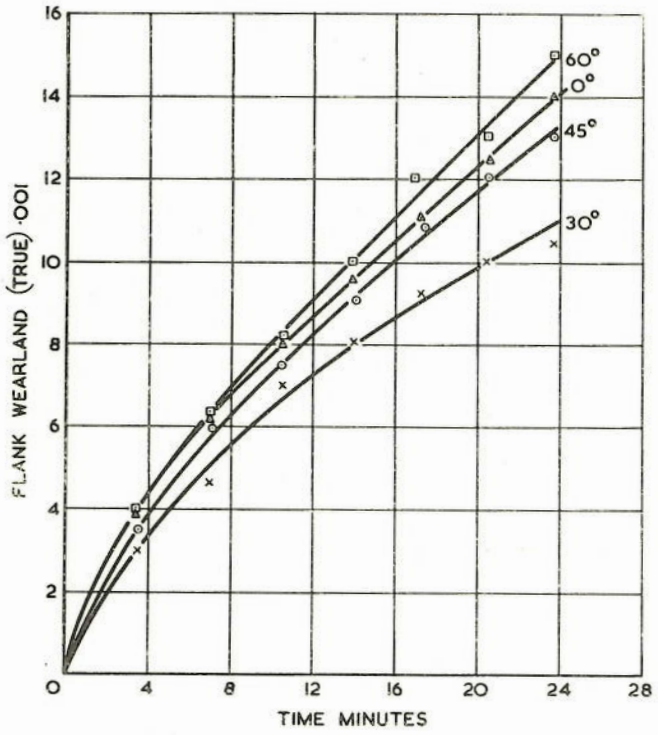

FIG.28. WEAR TESTS
FLANK WEARLAND (TRUE)
EN 8 TOOL No.4. END A

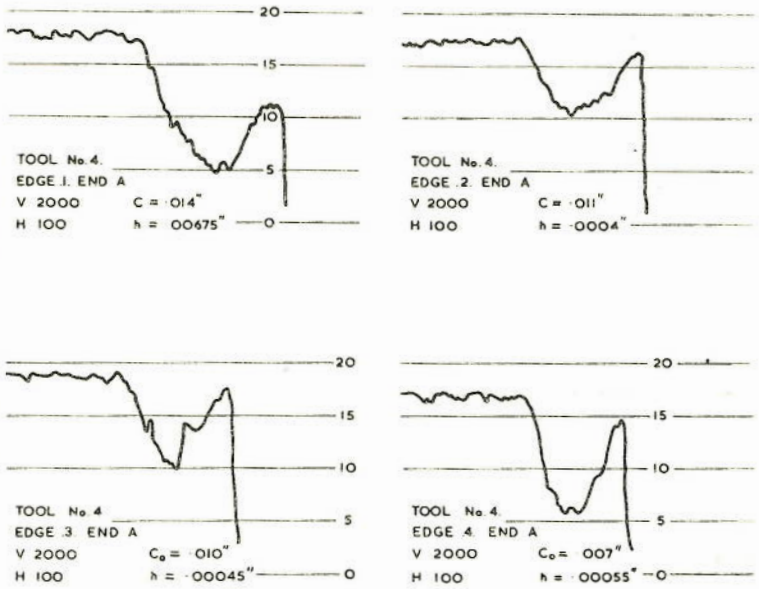

FIG.30. TALYSURF TRACES OF CRATER CONTOUR (SAMPLES).

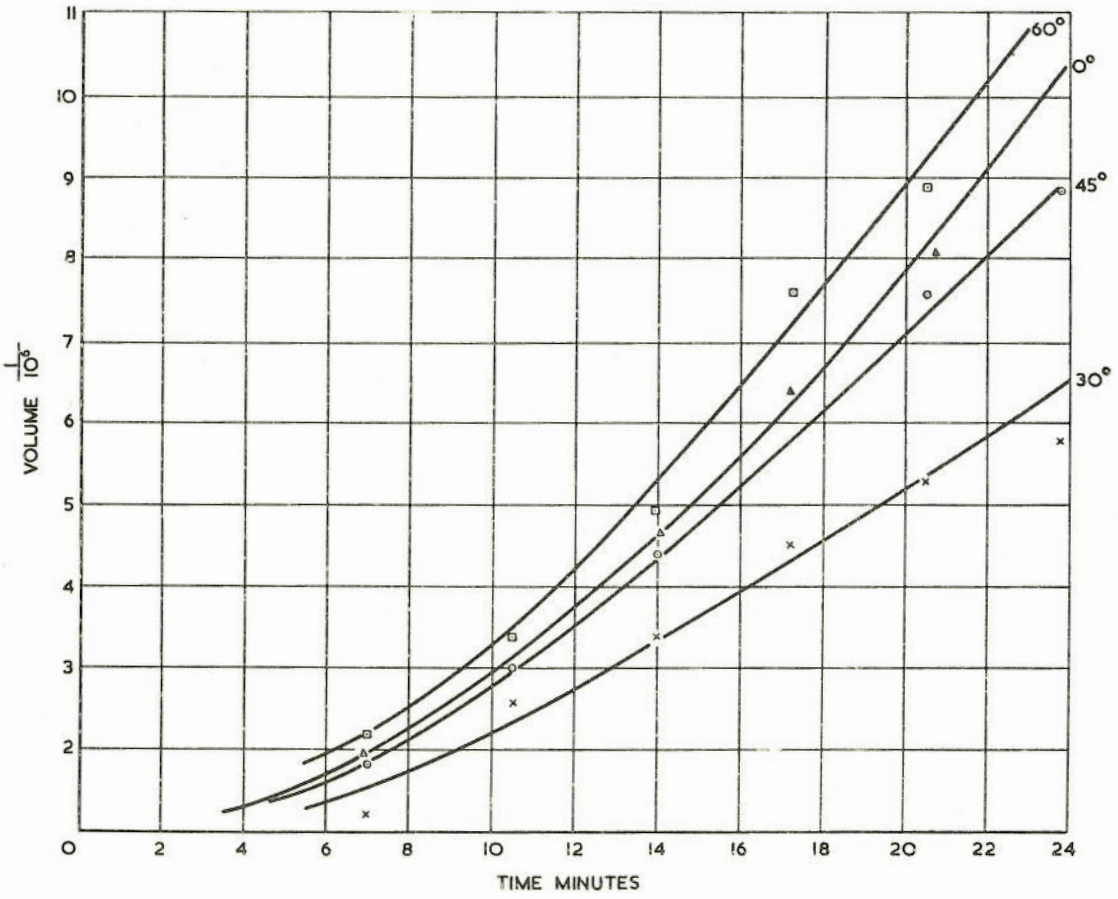

FIG.29. WEAR TESTS FLANK WEAR (VOLUME)
EN 8 TOOL No.4. END A.

FIGURE 31

Wear Tests

Crater Tool No. 4 End A

Summary of Results

		Edge 1 0°	Edge 2 30° (1.1547)	Edge 3 45° (1.4142)	Edge 4 60° (x2)
Time					
3.5 mins	Depth 'h'	.00015"	.0001	.0001	.0001
	Co	.014"	.010	.010	.008
	C	.014"	.0115	.014	.016
	Vol	1.87×10^{-6}"	$.99 \times 10^{-6}$	1.2×10^{-6}	2.4×10^{-6}
7 mins	Depth 'h'	.000225	.00015	.000175	.00015
	Co	.014	.010	.010	.008
	C	.014	.0115	.014	.016
	Vol	2.4×10^{-6}	1.96×10^{-6}	1.98×10^{-6}	2.53×10^{-6}
14 mins	Depth 'h'	.000375	.00025	.0003	.00035
	Co	.014	.0105	.010	.009
	C	.014	.012	.014	.018
	Vol	3.4×10^{-6}	2.3×10^{-6}	2.84×10^{-6}	3.85×10^{-6}
17.25 mins	Depth 'h'	.000425	.0003	.00035	.0004
	Co	.014	.0105	.010	.009
	C	.014	.012	.014	.018
	Vol	4×10^{-6}	2.65×10^{-6}	3.26×10^{-6}	4.9×10^{-6}
20.5 mins	Depth 'h'	.000575	.00035	.0004	.0005
	Co	.014	.0105	.010	.009
	C	.014	.012	.014	.018
	Vol	5.4×10^{-6}	2.75×10^{-6}	3.72×10^{-6}	6×10^{-6}
23.75 mins	Depth 'h'	.000675	.0004	.00045	.00055
	Co	.014	.011	.010	.009
	C	.014	.013	.014	.018
	Vol	6.3×10^{-6}	3.6×10^{-6}	4.14×10^{-6}	4.9×10^{-6}

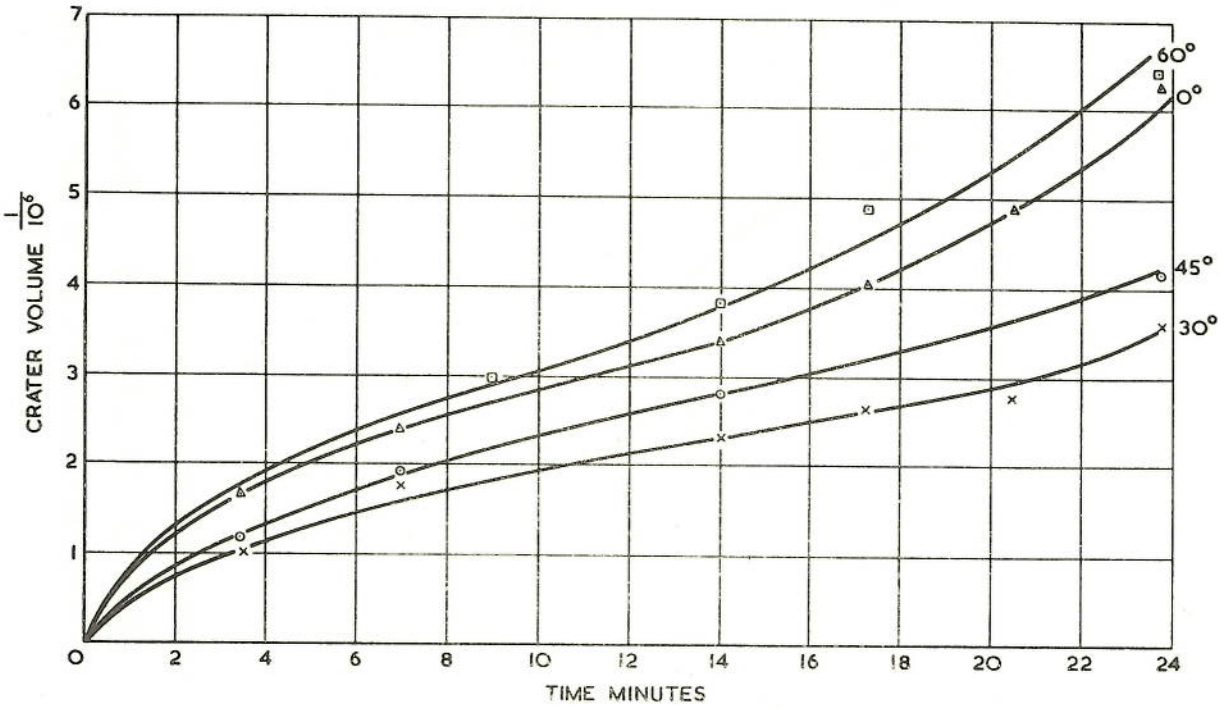

FIG.32. WEAR TESTS CRATER VOLUME Vs TIME
EN 8 TOOL No. 4. END A.

EN 8b TOOL T.C. WIMET XL 3
TIME INTERVALS 3·5, 7, 14, 17·25, 20·5, 23·75. MINS
SCALE – HORIZONTAL 1cm = ·001"
VERTICAL 1cm = ·0005"

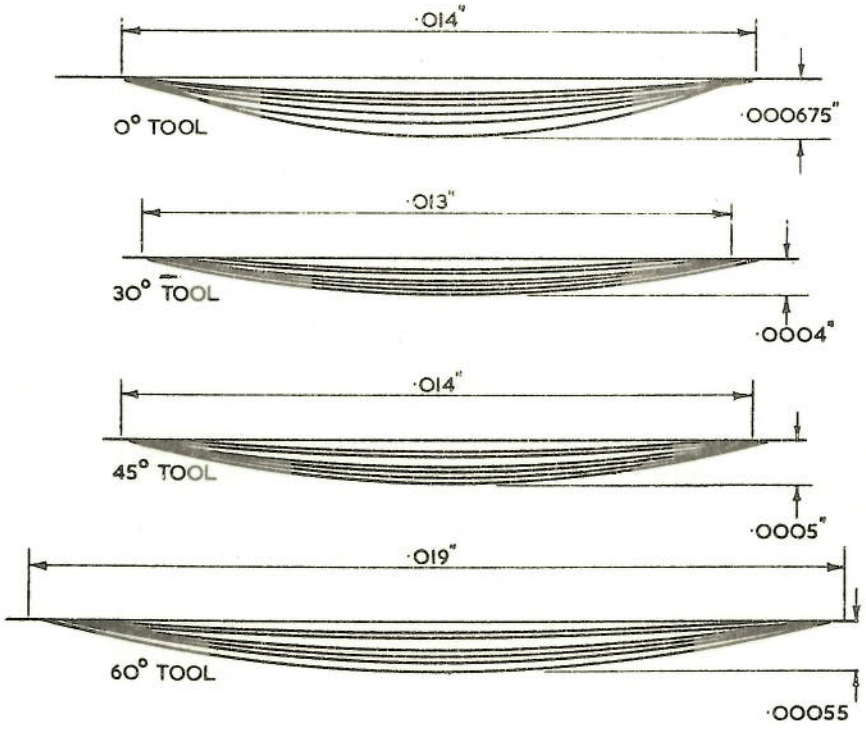

FIG .33. PICTORIAL GROWTH OF CRATER WEAR.

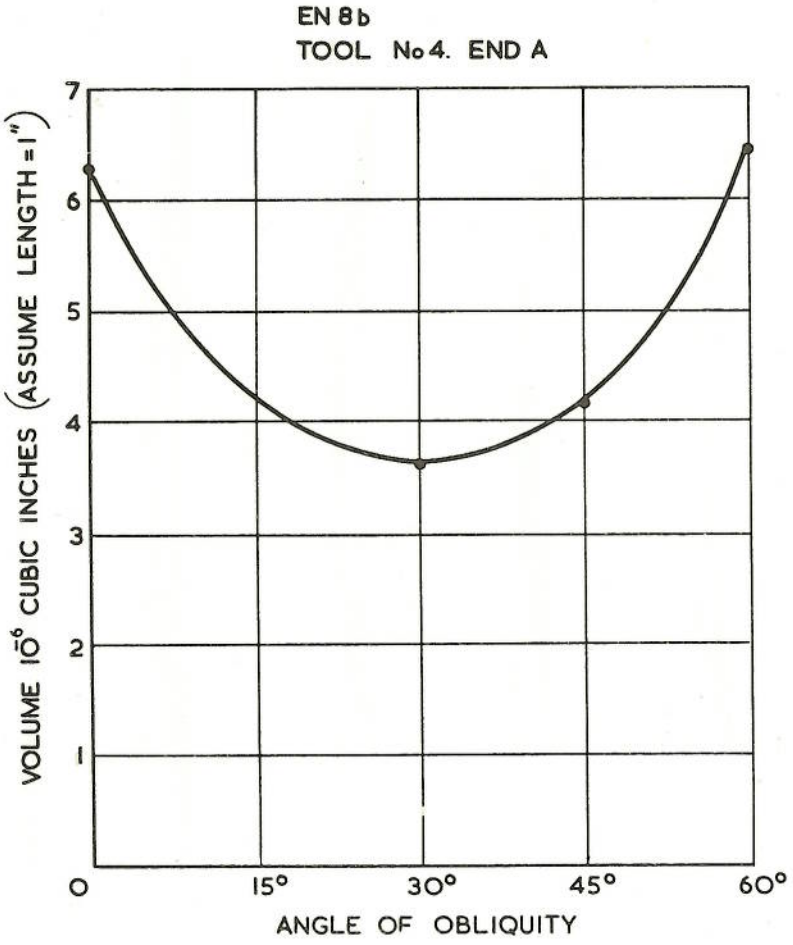

FIG.34. VOLUME OF METAL REMOVED AFTER 23·75 MINS. Vs ANGLE OF OBLIQUITY.

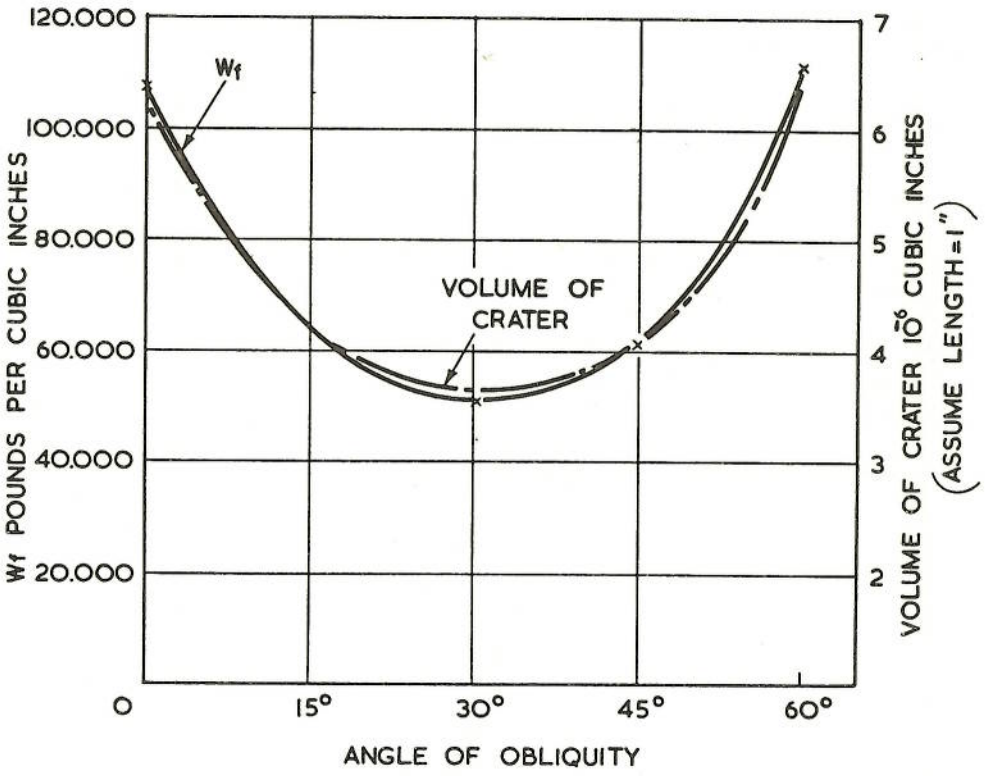

FIG.35. COMPARISON OF CURVES
WORK DONE IN FRICTION Wf (·0025)
AND VOLUME OF CRATER REMOVED AFTER 23·75 MINS

FIGURE 36.

Summary of Cutting Forces and Work done in Friction.

EN9 Speed 70 F.P.M. Feed .0025 Wall .068"

Obliquity	V F_c		S F_t		R F_L		Work done in Friction W_f
	Defl	lbs	Defl	lbs	Defl	lbs	
0°	5	41	6.5	27	0	0	132156 lbs/cu.ins.
30°	5	41	7	27	6.33	12	66017 "
45°	5.33	43	6.6	26	12	23	71714 "
60°	6.7	55	6.8	27	19,7	38	137026 "

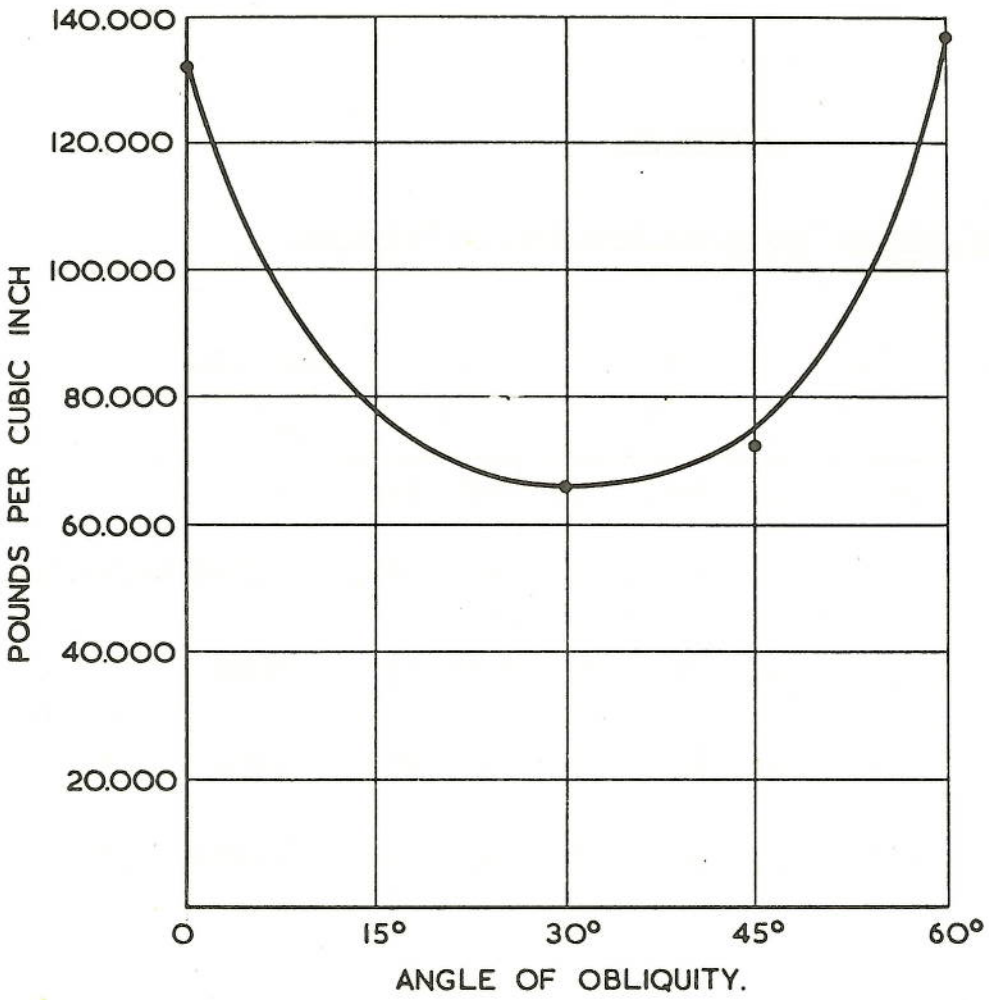

FIG.37. WORK DONE IN FRICTION Wf
EN9 FEED ·0025

Wear Tests EN9
Crater Tool No. 4 End B
Summary of Results
Edge 1
0°

Time	
2m 45 secs	h = .00015 C = .014 Vol = 1,87 x 10^{-6}
8m 15 secs.	h = .0003 C = .014 Vol = 2.84 x 10^{-6}
10m 5 secs.	h = .000375 C = .014 Vol = 3.4 x 10^{-6}
11m 55 secs.	h = .00045 C = .014 Vol = 4.14 x 10^{-6}

FIGURE 38

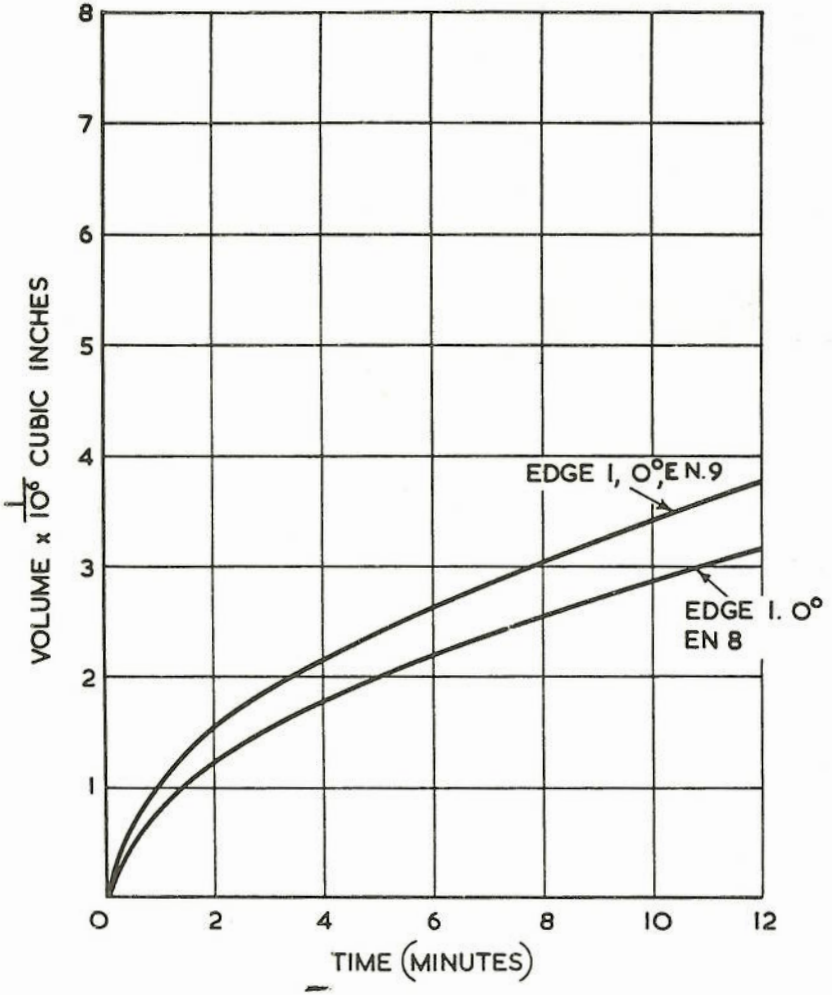

FIG. 39. WEAR TESTS
CRATER VOLUME EN 9 TOOL No. 4 END B.

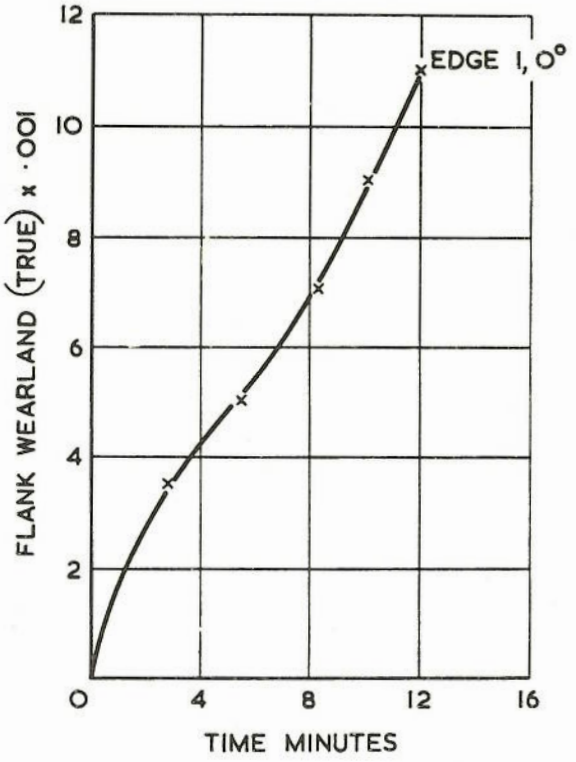

FIG. 40. WEAR TESTS
FLANK WEARLAND (TRUE)
EN 9 TOOL No. 4. END B